ELSEVIER

CrossMark

Patterning mechanisms of the sub-intestinal venous plexus in zebrafish

Michela Goi, Sarah J. Childs *

Department of Biochemistry and Molecular Biology and Alberta Children's Hospital Research Institute, University of Calgary, 3330 Hospital Drive NW, Calgary, AB, Canada T2N 4N1

ABSTRACT

Despite considerable interest in angiogenesis, organ-specific angiogenesis remains less well characterized. The vessels that absorb nutrients from the yolk and later provide blood supply to the developing digestive system are primarily venous in origin. In zebrafish, these are the vessels of the Sub-intestinal venous plexus (SIVP) and they represent a new candidate model to gain an insight into the mechanisms of venous angiogenesis. Unlike other vessel beds in zebrafish, the SIVP is not stereotypically patterned and lacks obvious sources of patterning information. However, by examining the area of vessel coverage, number of compartments, proliferation and migration speed we have identified common developmental steps in SIVP formation. We applied our analysis of SIVP development to *obd* mutants that have a mutation in the guidance receptor PlexinD1. *obd* mutants show dysregulation of nearly all parameters of SIVP formation. We show that the SIVP responds to a unique combination of pathways that control both arterial and venous growth in other systems. Blocking Shh, Notch and Pdgf signaling has no effect on SIVP growth. However Vegf promotes sprouting of the predominantly venous plexus and Bmp promotes outgrowth of the structure. We propose that the SIVP is a unique model to understand novel mechanisms utilized in organ-specific angiogenesis.

1. Introduction

Organ-specific regulation of sprouting, migration, proliferation and vascular network establishment during angiogenesis is one of the less well understood aspects of vascular development (Geudens and Gerhardt, 2011). One important role of the vascular system is to deliver nutrients acquired from the mother, or from absorption from the digestive system, to tissues and organs. To do so, blood vessels need to be in close contact with embryonic nutrient sources. In the adult, digestive system vessels need to be organized in highly efficient vascular networks.

Here, we focus on the development of vessels in the sub-intestinal venous plexus (SIVP), a set of predominantly venous angiogenic vessels that initially obtain nutrients from the yolk and transfer them to the developing embryo body through the adjacent yolk syncytial layer (YSL), and that will later support the distribution of blood to the digestive system in the larva and adult fish (reviewed in Carvalho and Heisenberg, 2010; Donovan et al., 2000). The developing sub-intestinal venous plexus (SIVP) has been used as an easily visible vascular bed to screen for molecules

that influence angiogenesis including pro- or anti-angiogenic factors (Chan et al., 2012; Kuo et al., 2011; Nicoli et al., 2009, 2007; Nicoli and Presta, 2007; Raghunath et al., 2009; Serbedzija et al., 1999). However, the study of the effects of these molecules is limited by poor knowledge of SIVP development, including whether or not this venous plexus is similar to other vascular beds in its development.

Little is known about early development of visceral vasculature in any animal model system but an anatomical atlas suggests that in zebrafish the supraintestinal artery (SIA) that delivers blood, and the bilateral sub-intestinal veins that collect the blood from the digestive system, start to develop around 2 dpf (Isogai et al., 2001). The SIVP is suggested to sprout from the duct of Cuvier (future common cardinal vein) and connect to the posterior cardinal vein (PCV) (Isogai et al., 2001; Nicoli and Presta, 2007). Around 3 dpf, the SIVP which has extended on the large surface of the yolk ball, appears as a vascular basket with compartments delimited by veins. The most anterior part of the right and left SIVPs drain into the hepatic sinusoids of the liver through the two hepatic portal veins. At 4 dpf, with the reduction of yolk size as the embryo feeds on it, the left SIVP starts regressing and empties into the right SIVP. Later, the blood from the posterior gut will only use the right SIVP to reach the liver (Isogai et al., 2001). Given that this plexus vascularizes essential visceral organs, gross defects in SIVP

patterning are likely not compatible with life.

Extrinsic cues and intrinsic receptors guide the morphogenesis of the vascular system. Vascular endothelial growth factor A (VegfA) induces endothelial cell proliferation and migration while inhibiting apoptosis (Carmeliet et al., 1996; Liang et al., 2001; Shalaby et al., 1995). During intersegmental vessel (ISV) angiogenesis, *vegfA* is expressed mid-somite around the notochord in a gradient to attract the sprouting vessels while its receptor (*vascular endothelial growth factor receptor 2*, *vegfr2*) is expressed by the angioblasts (Fouquet et al., 1997). In the zebrafish, *vegfA* expression is induced by *sonic hedgehog* (*shh*) expression at the midline (Lawson et al., 2002). Together with Vegf, Notch signaling is necessary for arterial specification in the trunk, and for the decision to take on a tip (migratory, proliferative) or stalk (non-migratory, non-proliferative) identity in the developing intersegmental arteries of the zebrafish embryo (Siekmann and Lawson, 2007). Platelet-derived growth factor (Pdgf) signaling has also been reported to induce ISV sprouting (Wiens et al., 2010).

Venous sprouting can be easily studied in the fish as it is clearly visible in real time. Venous ISVs form through cellular emigration from the PCV (Isogai et al., 2003; Yaniv et al., 2006) to connect with the arterial ISVs and require VegfC/Flt4 signaling. *vegfC* ligand is expressed in the dorsal aorta (DA) and its receptor *flt4* (*vegfr3*) in the sprouting cells of the vein (Covassin et al., 2006; Hogan et al., 2009a, 2009b). Bone morphogenetic protein (Bmp) is an important cue for venous migration ventrally during formation of the caudal venous plexus (CVP). Interestingly, VegfA is not required for CVP sprouting suggesting a difference between arterial and venous sprouting in the formation of this bed (Wiley et al., 2011). Venous sprouting of the CVP is also sensitive to perturbation in prenylation (Choi et al., 2011) and Sphingosine-1-phosphate signaling. The S1P1 receptor is expressed in endothelial cells and inhibits filopodia formation to stabilize the vascular network. Absence or reduction of S1P1 in the CVP causes excessive filopodial extensions resulting in a fused plexus instead of the wild-type honeycomb-like structure (Ben Shoham et al., 2012; Mendelson et al., 2013). A third example of venous sprouting can be found in formation of the common cardinal veins which occurs by lumen ensheathment and is sensitive to *vegfC* levels (Helker et al., 2013). These examples highlight diverse mechanisms and cues for venous sprouting in different organs. Here we characterize the sprouting of a fourth venous bed the SIVP and find significant differences in the cues and morphology of its development to other venous beds.

Only a few mutants show growth defects in the SIVP. *out of bounds* (*obd*) mutants have a mutation in the angiogenic guidance receptor *plexinD1* and an overgrown SIVP (Childs et al., 2002). *obd* ISVs also show disrupted control of timing and direction of angioblast migration from the dorsal aorta and an altered and overgrown caudal vein plexus (Childs et al., 2002; Torres-Vazquez et al., 2004). Plexins are transmembrane semaphorin (Sema) receptors that provide guidance for migrating angioblasts, axonal guidance and pruning, sensory-motor circuit connectivity and immune system development (Gay et al., 2011). A model for Sema-PlexinD1 signaling suggests that integrin based adhesion is lost when PlexinD1 receptor is activated by ligand causing retraction of filopodia and cellular detachment from the extracellular matrix, thus restricting migration (Sakurai et al., 2010). In the trunk, *sema3* ligands are expressed in the somites and *plexinD1* in the endothelium. *plexinD1* expressing angioblasts receive a repulsive signal when they contact the somite thus limiting their pathway to the space between somites (Torres-Vazquez et al., 2004; Zygmunt et al., 2011). Semaphorin-PlexinD1 signaling also has a second function in promoting *delta-like 4* (*dll4*) expression in tip cells downstream of VegfA signaling and thereby altering the tip-stalk cell balance to limit angiogenesis (Kim et al., 2011).

SIVP development is affected by lipoprotein levels. Mutation in the microsomal triglyceride transfer protein (*mtp*) causes excessive angiogenesis in the SIVP resulting in defective yolk absorption. *mtp* is expressed in the zebrafish yolk syncytial layer (YSL) and in the larval/adult gut and is important for the proper production of ApoB-containing lipoproteins (such as LDLs) that deliver lipids (Avraham-Davidi et al., 2012; Hussain et al., 2008; Marza et al., 2005). Low concentrations of lipoproteins decrease levels of *sflt1*, the soluble Vegfr1 (sFlt1) receptor. Since sFlt1 sequesters VegfA and therefore decreases signaling through Vegfr2 the end result is to enhance angiogenic sprouting (Avraham-Davidi et al., 2012; Kendall and Thomas, 1993; Roberts et al., 2004; Zygmunt et al., 2011). Interestingly, the intestinal lymphatics also grow in close relationship with the SIVP, may also have a role in lipid transportation, and may share similar signaling control (Okuda et al., 2012).

Using live imaging we trace SIVP development in real time. We find that the features of the developing SIVP are not hard-wired as they are in some other vascular beds of the zebrafish. The SIVP shows variable patterning among embryos, although we find common developmental morphologies. We identify commonalities in wild-type SIVP development in order to describe SIVP morphogenesis and apply it to the genetic *obd* mutants. Small molecule inhibition of the Vegf, Bmp and Mek/Erk pathways, but not other signaling pathways used in arterial growth, inhibit the proper formation of the SIVP. Our results suggest the developing gut vasculature responds to a unique set of growth factors, and is a model to shed insight into mechanisms of visceral organ angiogenesis.

2. Materials and methods

2.1. Zebrafish embryos

Embryos were collected and dechorionated through a brief treatment with pronase (Sigma-Aldrich, St. Louis, MO), incubated at 28.5 °C in E3 embryo medium and staged in hours post-fertilization (hpf) or days post fertilization (dpf). Endogenous pigmentation was inhibited from 24 hpf by the addition of 0.003% 1-phenyl-2-thiourea (PTU, Sigma-Aldrich) in E3 embryo medium. The fluorescent transgenic lines Tg(fli:EGFP)^{y1} (Lawson and Weinstein, 2002), Tg(fli:EGFP)^{y7} (Roman et al., 2002) were used to visualize cells and nuclei of endothelial cells respectively. *out of bounds* homozygous embryos *obd*^{fov01b} were used in all experiments using mutants (Childs et al., 2002). Morpholino knockdown (Gene Tools LLC, Corvallis, OR) used the following sequences: *bmp4* (5′-GTCTCGACAGAAAATAAAGCATGGG-3′) (Zeng and Childs, 2012), *vegfaa* (5′-GTATCAAATAAACAACCAAGTTCAT-3′) (Childs et al., 2002), *vegfab* (5′-GGAGCACGCGAACAGCAAAGTTCAT-3′) (Bahary et al., 2007) and *plexinD1* (5′-TGAGGGTATTTACAGTCGCTCCGC-3′) (Torres-Vazquez et al., 2004), at doses of 7, 2, 2 and 15.5 ng/embryo respectively.

2.2. Inhibitor treatments

Drug stocks were heated for 20 min at 65 °C and then diluted in E3 embryo medium and added to embryos from 4 or from 24 hpf. DMSO (D8418, Sigma) was used as a vehicle and control. Embryos were grown at 28.5 °C in the dark until imaging. Doses and sources are listed in Table S1.

2.3. Confocal imaging and measurements

Up to 10 embryos were mounted in 1% low melt agarose (Invitrogen) on glass bottom dishes (MatTek, Ashland MA) and imaged using a Zeiss LSM700 microscope using ZEN Black 2012
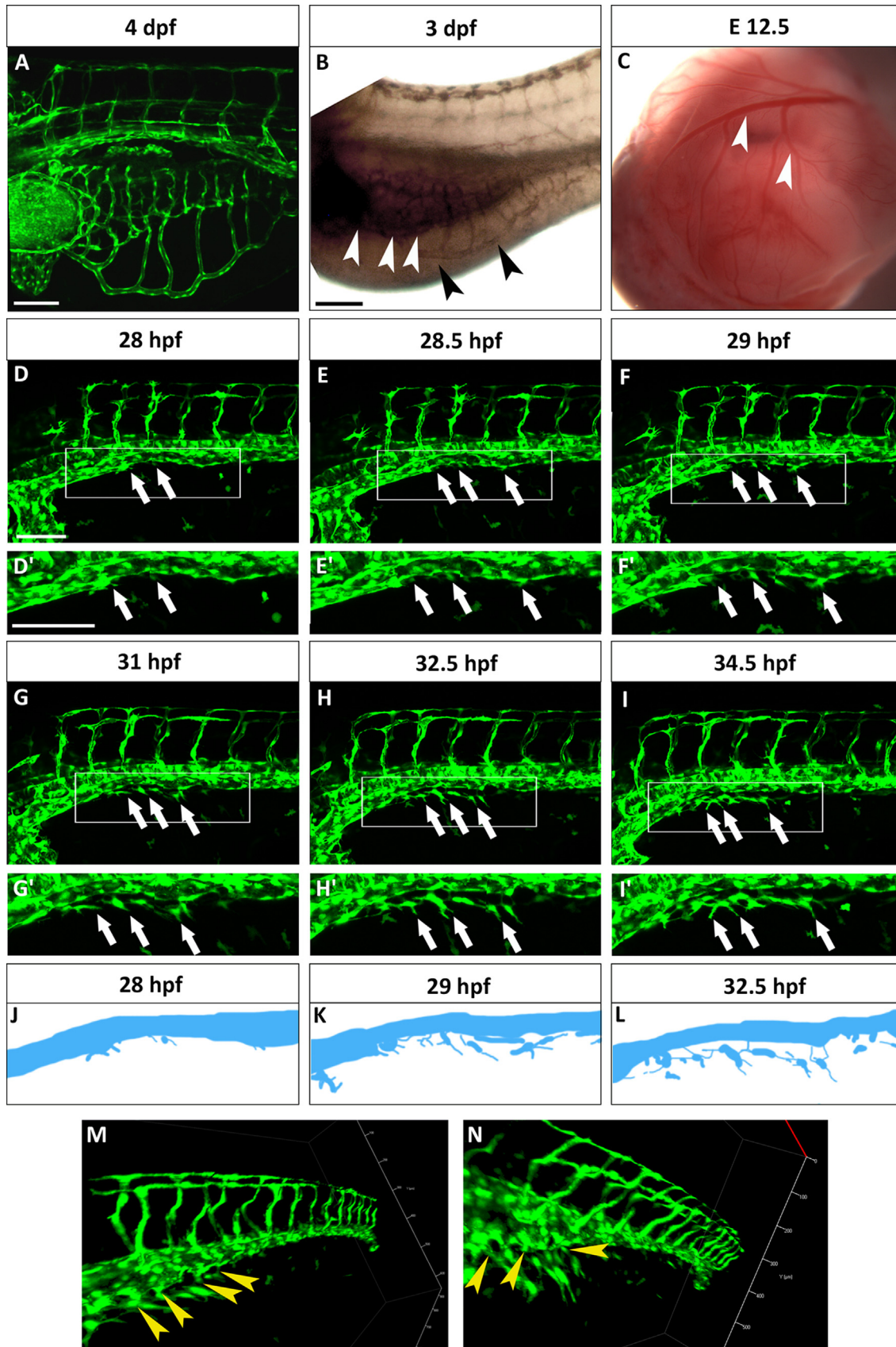
Fig. 1. The SIVP originates from the PCV. (A) Lateral view of a *Tg(fli:EGFP)^y1* zebrafish embryo at 4 dpf. The SIVP is located on the surface of the yolk. (B) *In situ* hybridization with *gata6* shows the position of the endoderm/gut (white arrowheads) in comparison to the outer SIVP basket (black arrowheads) at 3 dpf. (C) Analogous mouse omphalomesenteric vessels (vitelline veins) of the yolk sac of an E12.5 mouse embryo are indicated by white arrowheads. (D–I′) Single images taken from a time-lapse series highlight steps in the genesis of the SIVP. Images are shown for the left side of the embryo (D–E). At around 28 hpf, few cells start sprouting from the vein (white arrows). (F) At 29 hpf, the sprouts start elongating on the yolk ball (white arrows). (G–I) From 31 to 34.5 hpf, the SIVP continues to grow ventrally. (D′–I′Enlargements of embryos in D–I. (J–L) Schematics corresponding to specific time-lapse images (D′, F′, H′) that clarify the origin of SIVP vessels. (M–N) 3D images of the developing SIVP show sprouts emanating from the vein (yellow arrowheads). Scale bars represent 100 μm.

software (Carl Zeiss Canada Ltd). Slices 1–5 μm apart were gathered. For time-lapse, z-stacks were acquired every 30 min. ZEN Blue 2012 software was used for image processing and Fiji (Schindelin et al., 2012) for depth-coded pseudo-color of the stacks. For the calculation of area we considered the SIVP space delimited by veins below the same 5 somites. For the migration speed we measured the distance to the farthest point of the SIVP from the PCV at specific time points. A 2-tailed Student's *T*-Test or one way ANOVA test was run using SigmaPlot (Systat Software Inc., San Jose, CA).

2.4. In situ hybridization, antibody and EdU staining

Embryos were fixed in 4% paraformaldehyde (PFA, Sigma-Aldrich). Probe templates were produced by PCR amplification or using a plasmid template (Table S2). *In situ* hybridization was performed as described (Lauter et al., 2011). GFP was detected with a 1/500 dilution of anti-GFP antibody (Stratagene-Agilent, Santa Clara, CA) and by a secondary α-mouse biotin conjugated antibody and DAB staining (Vectastain, Vector Laboratories, Burlingame, CA). Invitrogen Molecular Probes Click-iT EdU Alexa Fluor 555 Imaging Kit (Eugene, Oregon, USA) was used to mark proliferative cells of the SIVP. EdU was incubated with the embryos for 30 min at 48 hpf. Embryos were mounted in 2% methylcellulose and were visualized under white light and photographed using a Stemi SV11 microscope, Axiocam HRc camera and AxioVision or ZEN Lite 2012 software or with a Zeiss LSM700 confocal microscope (Carl Zeiss Canada Ltd).

3. Results

3.1. Structural similarities between the zebrafish sub-intestinal venous plexus and mouse vitelline veins

The SIVP is a bilateral vascular structure (Fig. 1A and S1) in direct contact with YSL on the surface of the yolk (Carvalho and Heisenberg, 2010). The SIVP is therefore likely the vascular structure that mediates the uptake and circulation of nutrients from yolk to embryo (Isogai et al., 2001). The SIVP empties into the hepatic sinusoids of the liver using the two hepatic portal veins during early development (Isogai et al., 2001). The SIVP also forms the vascular plexus around the gut (Fig. 1B) that starts to circulate blood around 3 dpf before the left SIVP starts regressing around 4 dpf. Remodeling occurs so that posterior vessels connect to the right SIVP, which connects to the liver (Isogai et al., 2001).

The murine equivalent of the SIVP, the omphalomesenteric vessels (i.e., vitelline veins, Fig. 1C), belong to the extraembryonic circulation and connect the embryo with the yolk sac, transferring nutrients from the yolk sac to the circulation. These veins originate at 8 days post-coitum (dpc) from the blood islands, which are groups of mesodermal cells inside the yolk sac that form vessels by vasculogenesis (Kaufman, 1999a). The vitelline veins also initially provide blood supply to the embryonic digestive system and form hepatic sinusoids (Crawford et al., 2010; Kaufman, 1999a). At around 12.5 dpc, the right vitelline vein becomes the portal vein, which brings blood from the gut and spleen to the liver. The anterior part of this vein becomes the primitive inferior vena cava, while the extrahepatic portion of the left vitelline vein regresses (Crawford et al., 2010; Kaufman and Bard, 1999b). These connections and functions are similar to the pattern of zebrafish SIVP vessels.

3.2. The SIVP sprouts from the PCV

To gain insight into the early origin of the SIVP, we first

examined its development using confocal microscopy time-lapse of *Tg(fli:EGFP)^{y1}* transgenic embryos (Fig. 1D–F′ and Movie 1). We find that the SIVP first vessels start to form before 30 hpf. In contrast, previous studies using angiography suggested that these vessels form only at 48 hpf (Isogai et al., 2001) (Fig. 1D–D′). On the right side of the embryo, SIVP sprouting starts slightly later, giving rise to a less extensive basket (Fig. S1). Moreover, due to the fact that the right SIVP does not generate hepatic sinusoids it does not extend as far anteriorly (Fig. S1) (Isogai et al., 2001), all further data shown here is from the left side. Instead of seeing initial sprouts originating from the duct of Cuvier, as previously suggested (Isogai et al., 2001; Nicoli and Presta, 2007), we see sprouting from the posterior cardinal vein (Fig. 1D–F′, white arrows). 3D reconstructions confirm our observation (Fig. 1M and N). Anterior and posterior sprouts then migrate towards each other, join, continue to sprout, and grow ventrally to form a developed vascular basket above the yolk ball (Fig. 1D–I′) as schematized in Fig. 1J–L. To support our finding we analyzed the expression of arterial and venous markers, however they are not expressed highly enough in these vessels at this developmental stage to be informative (Fig. S2). While this paper was under revision, Nicenboim and colleagues suggested that the PCV cell population gives rise to the SIVP but also also gives rise to the SIA. It is possible that arteriovenous identity is not fully established in the PCV at this developmental stage (Nicenboim et al., 2015).

Supplementary material related to this article can be found online at http://dx.doi.org/10.1016/j.ydbio.2015.10.017.

3.3. The SIVP is not stereotypically patterned and has a superficial and deep plexus

We noticed that individual *Tg(fli:EGFP)^{y1}* embryos have different SIVP patterns over time, particularly from 2 to 4 dpf (two representative embryos are shown in Fig. 2). We note that the position and number of vessels is similar but not precisely the same (Fig. 2A–A′ and D–D′). This suggests that there is not a strict stereotypical control of the SIVP pattern as observed for the ISVs in the trunk, but there are physical or molecular patterning cues that guide the patterning into the basket shape. Moreover, we notice that the pattern continues to be variable during later development as the embryos continue to show differences in vessel path and number, number of compartments, area, and vessel branching (Fig. 2A–F′). While the early SIVP is superficial and located on the yolk surface, at 3 dpf there is a second inner vascular basket of vessels visible (white arrowheads in Fig. 2B–F′) which is connected to the outer basket through common vessels (red arrowheads in Fig. 2B', C', E' and F'), highlighted in the schematics (Fig. 2G). These connections are more apparent at 4 dpf as rendered in depth-coded pseudo-colored stacks (Fig. 2C–C′ and F–F′). Since the inner basket has close contact with the intestine and the outer basket regresses during development, we hypothesize that the inner basket will form the gut vasculature and hepatic sinusoids, while the external basket may serve to gather nutrition from the yolk in the early development.

3.4. The SIVP shows common developmental steps instead of a stereotypical pattern

To develop a staging series useful for comparison with mutants we observed common features of SIVP formation in different embryos between 30 and 80 hpf (Fig. 3 and Movie 2). At 30 hpf we see the first SIVP vessel along the body of the embryo (Fig. 3A). At 34 hpf we see the sprouting of the first SIVP vessel from both directions to make what will become the outer basket (Fig. 3B). Compartments (defined as vascular honeycomb-shaped structures) form at around 48 hpf (Fig. 3C). At 55 hpf filopodia are
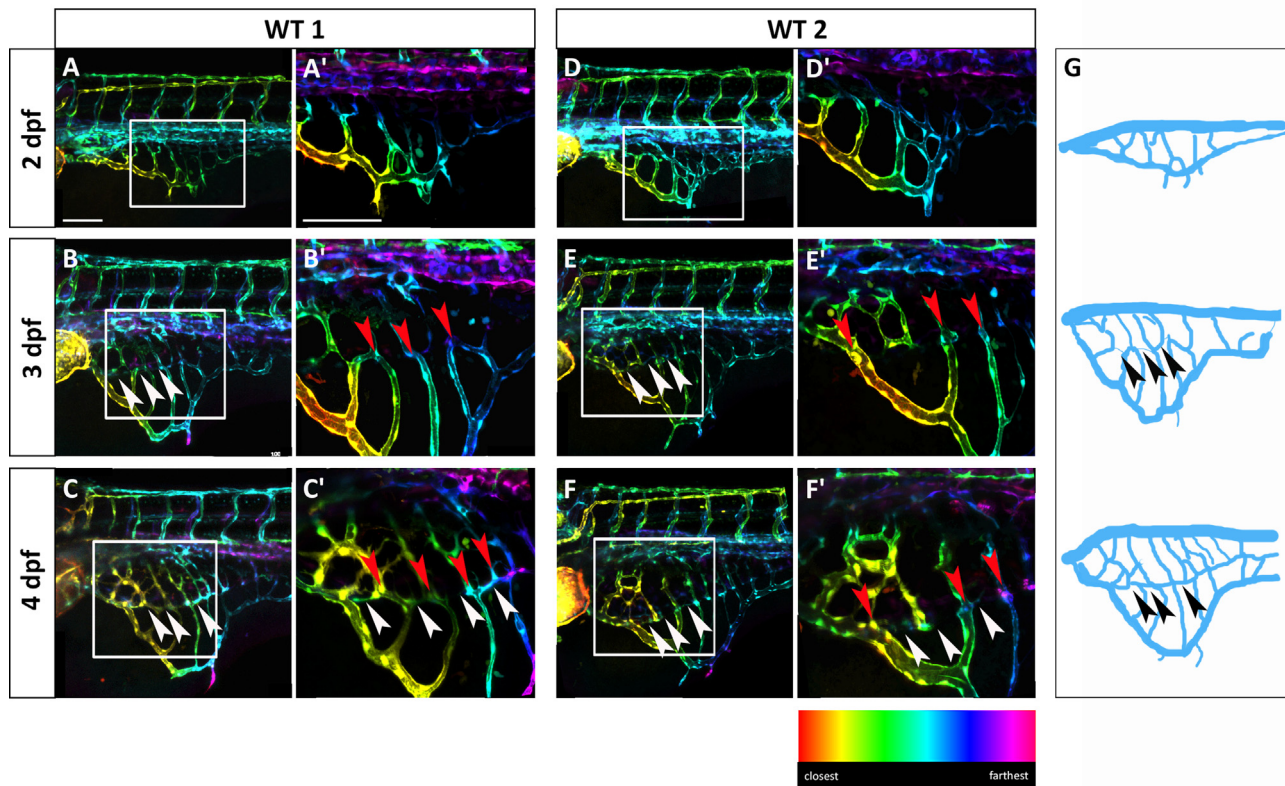
Fig. 2. The SIVP vascular pattern is variable among embryos and develops superficial and deep vessel baskets. Depth-coded confocal Z-projections of SIVP development in two individual embryos (A–C′ and D–F′) from 2 to 4 dpf show a similar organization, but small differences in pattern. (A, D) At 2 dpf, the SIVP appears as a single basket on the surface of the yolk. (B, E) At 3 dpf a deeper second vascular basket is visible (the border of the inner basket is indicated by white arrowheads). (C, F) This inner basket becomes more evident at 4 dpf. Some vessels connect both inner and outer vessels (red arrowheads). (A′–F′) Enlargements of images in A–F. (G) Schematics from WT 1 embryo images A–C. Arrowheads indicate the boarder of the inner basket. Scale bars represent 100 μm.

clearly evident extending from the forming SIVP in an active cue search as the structure grows ventrally (Fig. 3D). Around 58 hpf lamellipodia are more prevalent at the leading edge of the ventral migration (Fig. 3E). Migration continues at 65 hpf (Fig. 3F), and the continuing expansion of the SIVP on the yolk ball occurs in parallel with the onset of remodeling and pruning of some vessels (Fig. 3G and H; blue arrows in F′–H′). These common steps define a staging series of SIVP formation (schematized in Fig. 3I) and are useful to understand developmental restrictions in a vessel bed that does not have a 'hard-wired' pattern.

Supplementary material related to this article can be found online at http://dx.doi.org/10.1016/j.ydbio.2015.10.017.

3.5. Quantification of SIVP growth and pattern

We next developed a quantitative metric that describes the SIVP developmental process and allows meaningful comparison with mutants. We were careful to control for potentially confounding variables in our imaging and analysis. Firstly, each embryo was positioned dorso-laterally in order to obtain stereotypical images that were not distorted by the rounded nature of the yolk ball. Secondly, we used anatomical landmarks, such as the angle of the right and left dorsal longitudinal anastomotic vessels (DLAVs) in the anterior part of the trunk, to ensure that the area captured of different embryos was comparable. By studying a number of embryos, and analyzing only embryos with an entirely visible SIVP, we reduced error from these sources.

We calculated the area of vessel coverage at two different stages, 55 and 80 hpf (Fig. 4A). These stages were chosen because they are representative of two phases of SIV expansion and development, and are in a time window when angiogenic defects become evident in mutants. We measured the area of the SIVP below the same 5 somites at 55 hpf and obtained a mean area of $35,866 \pm 7023$ μm^2 ($n=18$) for the SIVP. At 80 hpf the mean area reached $56,128 \pm 8585$ μm^2 ($n=23$ embryos; Fig. 4A).

To measure migration speed, the farthest extent of migration of the SIVP outer basket was tracked in 5 embryos from 30 to 80 hpf in time-lapse and the migration distance was calculated as the distance to the farthest point of the SIVP at specific time points from the posterior cardinal vein (Fig. 4B). We found that the average speed of migration was as 4.5 ± 0.6 μm/h. We find that there are an average of 11 ± 2.3 ($n=17$) vessel compartments within the SIVP at 55 hpf (Fig. 4C). Using the average SIVP area the average area of a compartment is 3260 μm^2. The number of compartments could not be calculated for 80 hpf because it was difficult to resolve individual compartments once inner and outer baskets developed.

3.6. Both leading and trailing cells proliferate during migration

In mouse retina, stalk cells proliferate but tip cells do not (Gerhardt et al., 2003) while in zebrafish intersegmental arteries, tip cells proliferate but not stalk cells (Siekmann and Lawson, 2007). We tracked cell division in the SIVP in time-lapse in individual *Tg(fli:EGFP)*^{y7} embryos, which express the transgene only in the nuclei of endothelial cells, allowing us to track cell division events (Movie 3). From 46 to 50 hpf in the SIVP, we find proliferation of tip (leading) and stalk (trailing) cells during the expansion of the vascular basket (Fig. 5). Thus we find comparable cell division throughout the SIVP, with no preference for either tip or stalk. This conclusion is also supported by EdU staining (Fig. 5I–K″′).
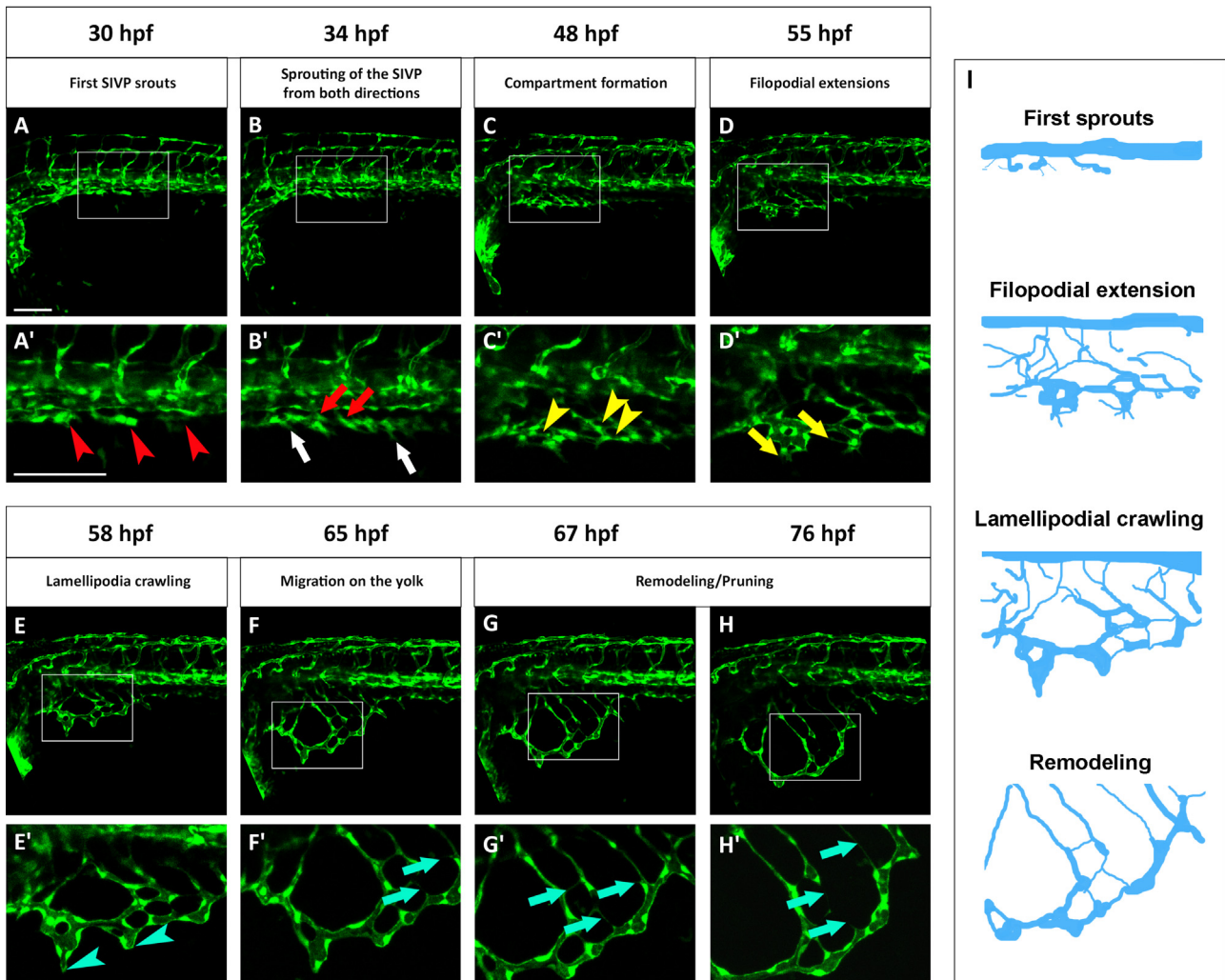
Fig. 3. Standardized staging series for SIVP development. Representative confocal micrographs of a time-lapse of SIVP development chosen to show common steps between 30 and 76 hpf. (A′–H′) Enlargements of images below each single original frame. (A′) Red arrowheads indicate the sprouts from the PCV. (B′) Red arrows indicate the sprout from the first SIVP vessel connecting with the supraintestinal artery, located along the midline. White arrows indicate the sprouts from the first SIVP vessel migrating ventrally around the yolk. (C′) Yellow arrowheads point to developing compartments. (D′ Yellow arrows mark the presence of filopodia. (E′) Blue arrowheads show the formation of lamellipodia. (F′–G′–H′) Blue arrows indicate pruning events. (I) Schematics corresponding to key timepoints (A′, D′, E′ and G′) in the progression of SIVP development. Scale bars represent 100 μm.

Supplementary material related to this article can be found online at http://dx.doi.org/10.1016/j.ydbio.2015.10.017.

3.7. obd mutants show excessive SIVP angiogenesis

obd zebrafish develop precocious and spatially unrestricted arterial ISV sprouts, anomalous angioblast migration, and ectopic connection among vessels (Childs et al., 2002). Interestingly, the SIVP also has an anomalous pattern in *obd* mutants (Fig. 6), suggesting PlexinD1 involvement in SIVP patterning. PlexinD1 is expressed in SIVP endothelial cells (Fig. S1). Putative PlexinD1 ligands are expressed very weakly at this developmental stage in the yolk region and we could not determine which was likely to be the PlexinD1 ligand for patterning (Fig. S1). We examined SIVP formation in *obd^{fov01b}*; *Tg(fli:EGFP)^{y1}* embryos or *plexinD1* morphants as compared to wild-type *Tg(fli:EGFP)^{y1}* embryos, employing our wild-type staging series.

Confocal microscopy time-lapse of *obd* mutant embryos reveals that SIVP patterning is more variable among individual *obd* mutants than among wild-type embryos (Fig. 6). We observe an increased number of compartments, greater expansion on the yolk and a higher number of sprouts from the basket in *obd* mutants. This suggests that the molecular restrictions establishing a regular SIVP cannot control the growth in the *obd* mutant (schematics, Fig. 6G–I). The inner basket and its connections to the outer basket are visible (Fig. 6B–F′).

Using our staging series, we observe common features in SIVP formation in individual *obd* mutant embryos but they were accompanied by excessive vascular growth (Fig. 7 and Movie 4). The first SIVP vessel sprouts precociously in *obd* mutants (Fig. 7A–A′) as compared to wild-type embryos (Fig. 3A–A′). The fast expansion of the plexus is driven by increased and constant sprouts from the inner connecting vessels and new sprouts from the PCV (Fig. 7C–D′). Filopodia are present during the entire SIVP expansion, with
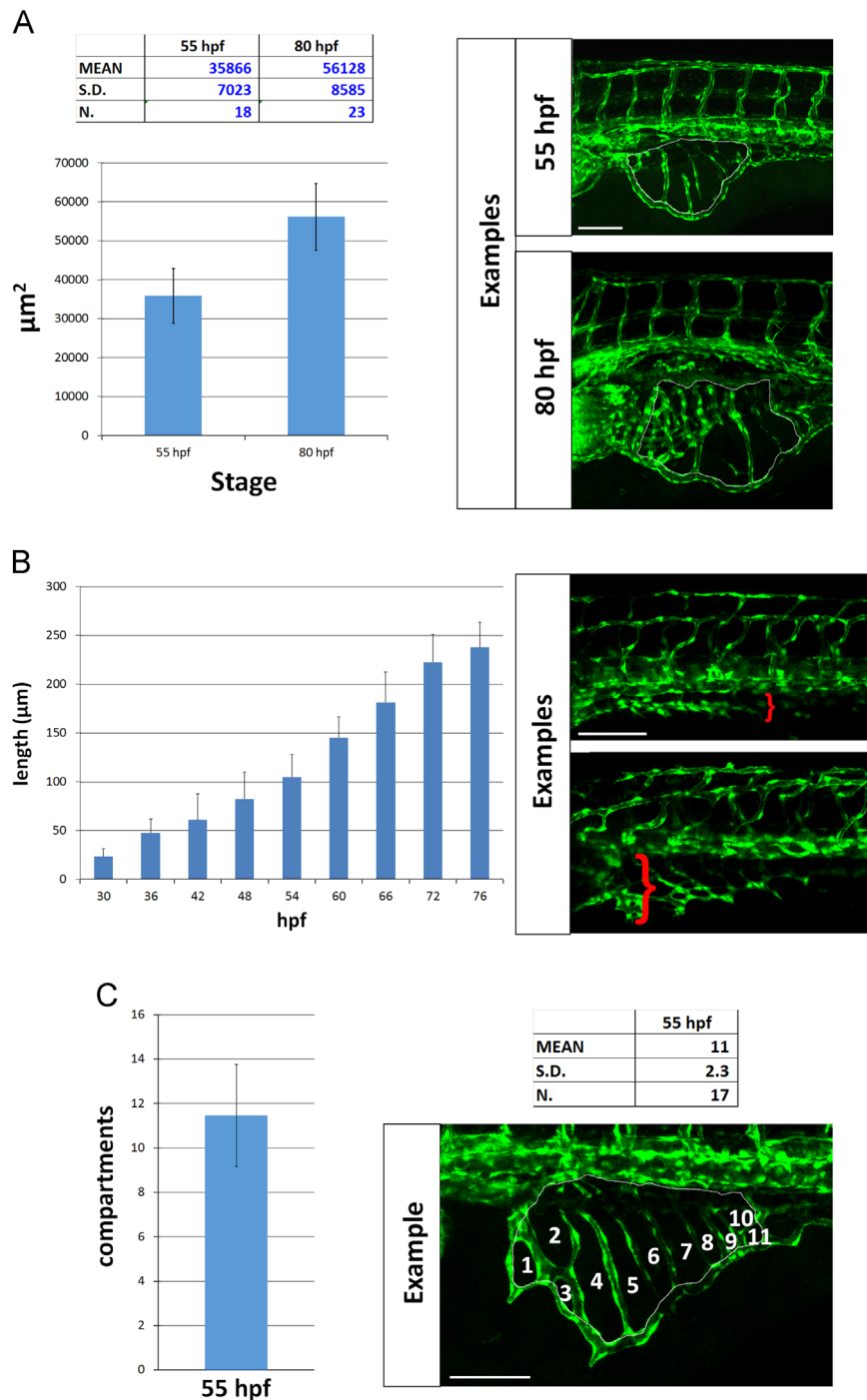
Fig. 4. Quantitative analysis of SIVP vessel angiogenesis in wild-type embryos. (A) Measurement of the area of the vessel coverage over the yolk at two different stages. (B) The extent of migration of the SIVP outer basket was tracked from 30 to 76 hpf in multiple embryos. The average values were calculated and plotted in a graph. (C) The mean number of compartments per SIVP was calculated at 55 hpf. Scale bars represent 100 μm.

thin processes developing from pre-existing vessels even at 76 hpf. Significantly, no pruning events were observed (Fig. 7E–H′).

Supplementary material related to this article can be found online at http://dx.doi.org/10.1016/j.ydbio.2015.10.017.

The SIVP expands on the yolk more than wild-type (compare Figs. 7I and 4A) and measured 37,268 $\pm$ 6341 μm^2 (n=24 embryos), significantly larger than wild-type embryos at 33,128 $+/-$ 6591 μm^2 ($p < 0.05$; Fig. 9A). Moreover, there is a striking difference in small angiogenic vessels forming compartments. *obd* mutants show a mean of 30 compartments *versus* 11 compartments present in wild-type embryos ($p < 0.01$, Fig. 7J).

A previous study demonstrates that the absence of Sema-PlexinD1 signaling in *obd* mutants results in more endothelial cells within the ISV sprouts and in more tip cells compared to wild-type embryos (Zygmunt et al., 2011). Here, we observed a higher number of sprouts to form the SIVP in *obd* mutants and by analyzing proliferative cells during SIVP expansion we detected proliferation of both tip and stalk cells in *plexinD1* morphants (Fig. S3; Movie 5). This conclusion is also supported by EdU staining (Fig. S3).

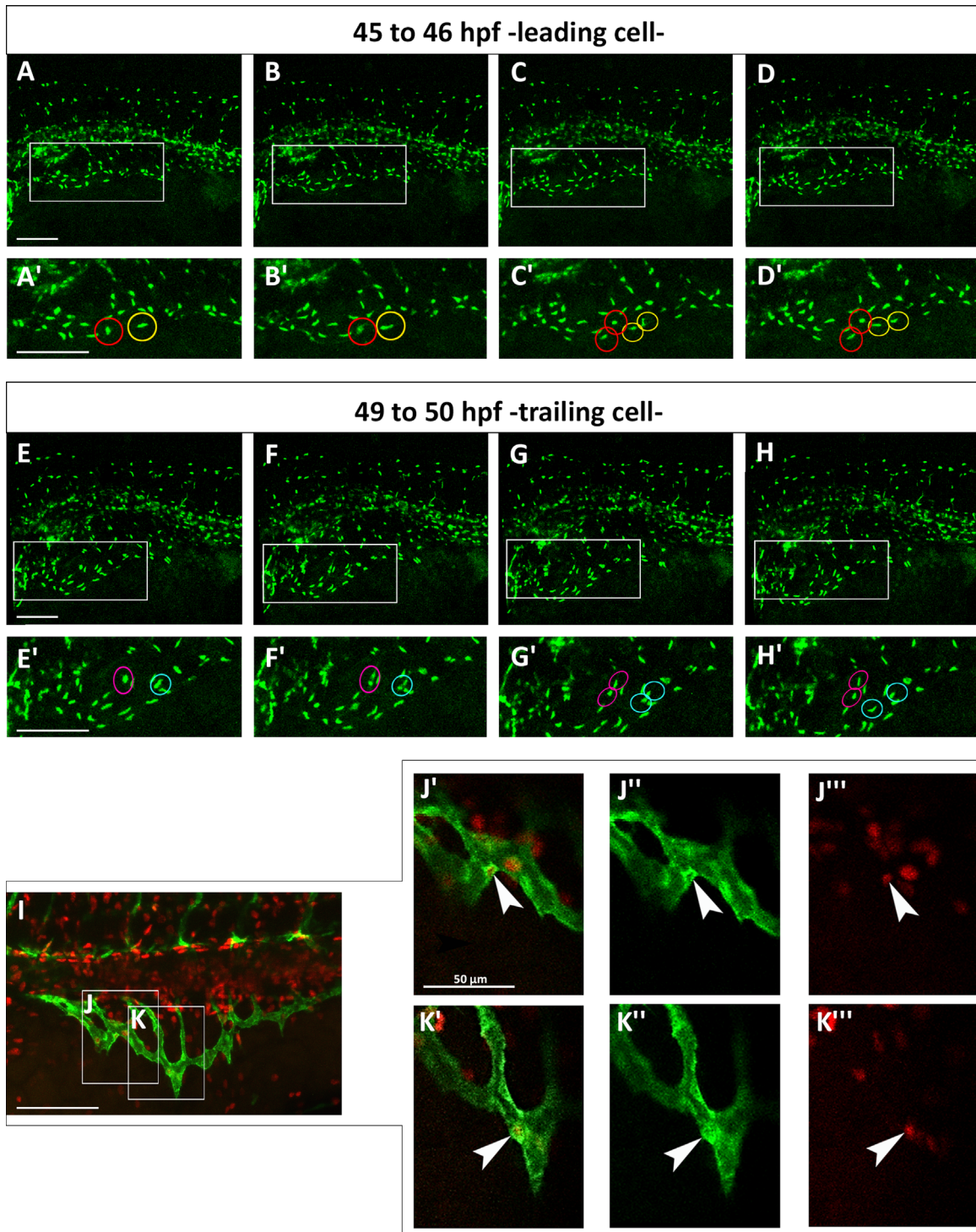Supplementary material related to this article can be found online at http://dx.doi.org/10.1016/j.ydbio.2015.10.017.

Fig. 5. Both leading and trailing cells proliferate during migration. (A–H) Confocal micrographs of a time-lapse of a *Tg(fli:EGFP)^y7* embryo. (A′–H′) Enlargements are shown below each frame. (A′–D′) Red and yellow circles indicate two proliferating leading cells from about 45 to 46 hpf. (E′–H′) Magenta and blue circles indicate two dividing trailing cells from about 49–50 hpf. (I) Red EdU staining on *Tg(fli:EGFP)^y1* embryo at 48 hpf. (J–K) Boxes indicate the position of the enlargements from image I. J indicates a trailing cell and K a leading cell. (J′–K‴) Merge of enlargement of boxes J and K. Endothelial cells are marked green and proliferating nuclei, red. White arrowheads indicate SIVP proliferating cells. Scale bars represent 100 μm.

3.8. Vegf and Bmp pathways promote SIVP development in parallel

We next wanted to understand the growth factor and guidance cues that set up the migration and pattern of the SIVP. Given that the development of arterial vascular beds is controlled by a number of growth factors and that venous sprouting requires a different set of cues, we tested whether any of these factors are important in SIVP formation. We undertook a screen using small molecule inhibitors adding them in E3 embryo medium at 24 hpf before the first sprouts form the first SIVP vessel.

We found several signaling pathways had no effect on SIVP development. While Notch signaling controls angiogenic cell behavior in the intersegmental arteries (Siekmann and Lawson, 2007), inhibiting Notch with 100 μM DAPT or 25 μM LY411575 did
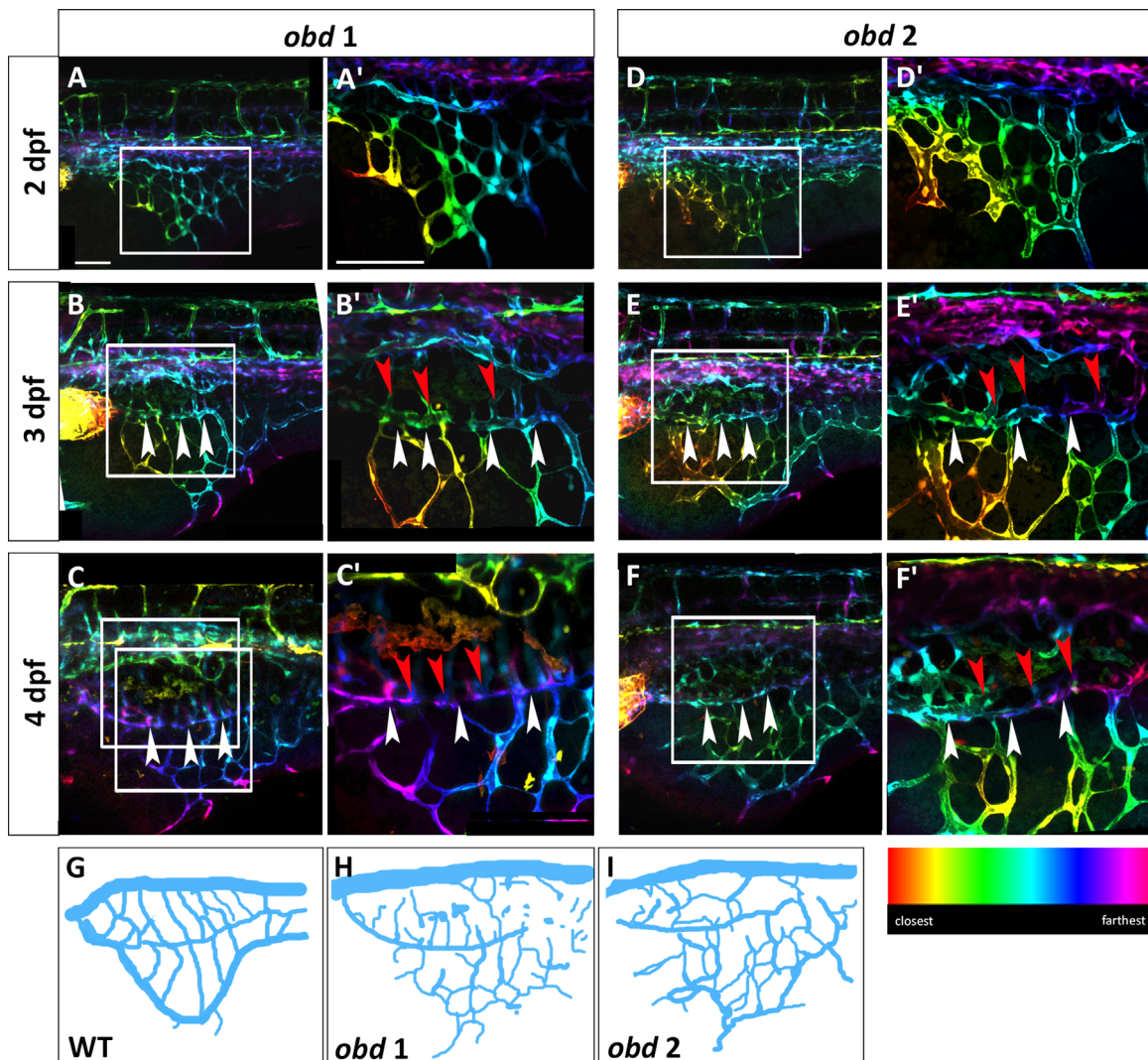
Fig. 6. *obd* mutants have a variable SIVP pattern and SIVP overgrowth. Depth-coded confocal stacks of SIVP development in two individual embryos (A–C′ and D-F′) of *obd*fov[01b]; *Tg(fli:EGFP)[y1]* line from 2 to 4 dpf showing variability in SIVP pattern. The border of the inner vascular basket is indicated by white arrowheads. Shared vessels between the inner and outer basket are indicated by red arrowheads. Scale bars represent 100 μm. (G–I) Schematics of SIVP phenotype in wild-type (Fig. 2C), *obd 1* (Fig. 6C) and *obd 2* (Fig. 6F) embryos at 4 dpf.

not affect SIVP development (Fig. S4). These drugs elicited other documented phenotypes such as an upwardly curled body axis suggesting the drugs were functional (Fig. S5). Thus Notch activity does not appear to be involved in SIVP formation.

Sonic hedgehog signaling also appeared to play no role in SIVP development. *shh*, expressed in the early mouse gut endoderm, plays a role in gut, liver, villus and smooth muscle morphogenesis (Ramalho-Santos et al., 2000; Wallace and Pack, 2003; Zeng and Childs, 2012). Moreover, Shh induces the expression of *vegfaa* in the somites, which is important for ISV development (Lawson et al., 2002). However, blocking *shh* with 50 μM cyclopamine, a hedgehog receptor inhibitor (Fig. S4) did not alter SIVP development suggesting that Shh does not control SIVP formation. We verified the function of cyclopamine by looking for hemorrhage and curly-down body axis in drug treated embryos as shown in Lamont et al., 2010 (Fig. S5–6).

Platelet-Derived Growth Factor (Pdgf) also appears to play no role in SIVP growth or patterning. Pdgf signaling promotes ISV angiogenesis (Wiens et al., 2010). Pdgf is a potent mitotic inducer with two receptors, Pdgfrα and Pdgfrβ, both inhibited by 0.25 μM Pdgfr Inhibitor V (Wiens et al., 2010). We found that Pdgfr Inhibitor V treated embryos showed a lack of inner compartment

formation in the SIVP, an identical phenotype as seen for Vegfr2 inhibition suggesting a possible function of Pdgf signaling in SIVP development (Fig. S4). However, Pdgfr Inhibitor V (also called Ki 11502) has reported activity on the Vegfr2 (Nishioka et al., 2008) and thus we tested a second Pdgf receptor inhibitor (imatinib). 50 μM imatinib did not affect SIVP development (Fig. S4). This observation suggests that the absence of internal vessels detected with Pdgfr Inhibitor V exposure is caused by its activity on Vegfr2 rather than by the specific action on Pdgfr. This conclusion is also supported by the presence of CtAs in imatinib treated embryos and their absence when Pdgfr Inhibitor V was used (Fig. S6).

On the other hand, two pathways strongly affected SIVP development. The Bmp pathway is important for gut smooth muscle formation (Kedinger et al., 1998; Roberts et al., 1998), and is also necessary for formation of a closely related venous vessel bed in zebrafish, the CVP (Wiley et al., 2011). *bmp4* is expressed in the gut during SIVP development while *alk2* transcript is detectable in the axial vessels (Fig. S1) (Roman et al., 2002; Zeng and Childs, 2012). 50 μM DMH1 (inhibitor of the Bmp type I receptor Alk2; Hao et al., 2010) caused a reduction of the SIVP expansion but did not ablate or disrupt the pattern of the SIVP, suggesting that Bmp plays a role in outgrowth but not patterning (Fig. 8C–C′). To test that this dose
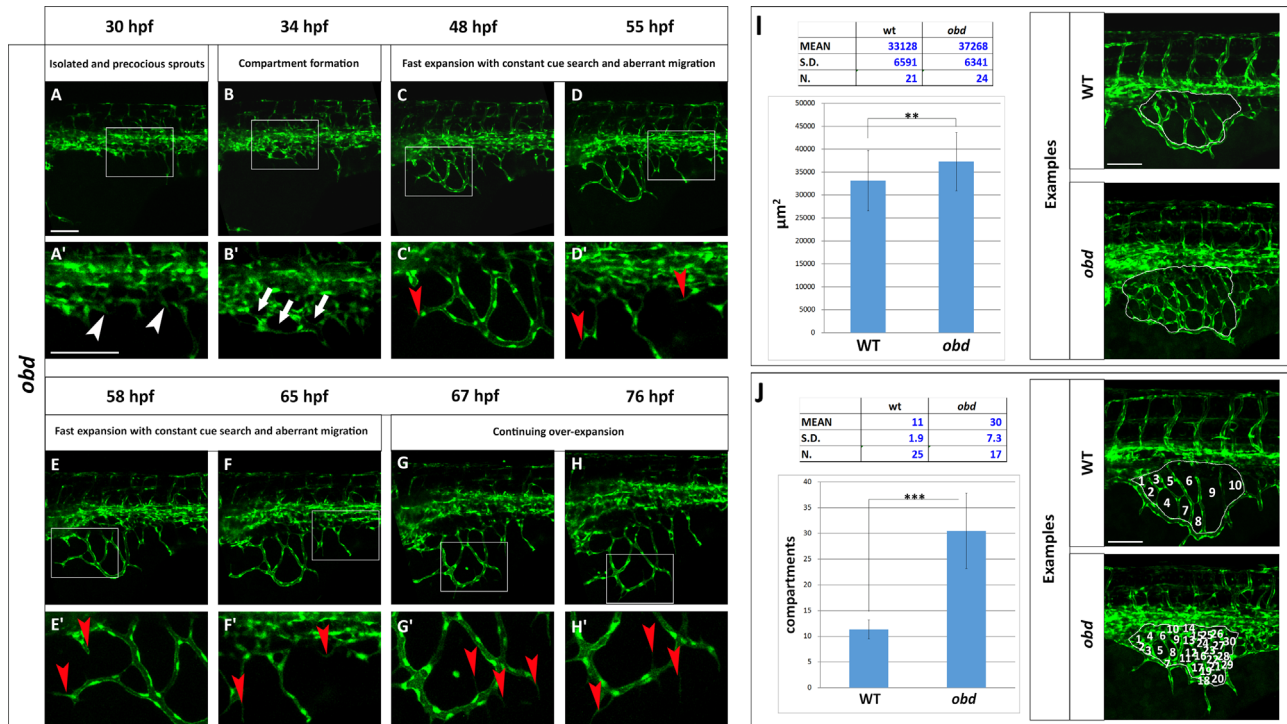
Fig. 7. The *obd* SIVP shows precocious development, constant cue search, aberrant migration and higher number of compartments. (A–H) Confocal micrographs from a time-lapse of a developing *obd*[fov01b]; *Tg(fli:EGFP)*[y1] SIVP. (A′–H′) Enlargements of images in A–H. (A′) White arrowheads indicate the precocious development of the SIVP vessels. (B′) White arrows point to some of the developing compartments. (C′-D′-E′-F′) Red arrowheads mark the presence of constant filopodial extension and aberrant migration and sprouting. (G′-H′) Red arrows indicate the formation of new filopodia scanning the environment. No pruning events are visible. (I–J) Quantitative analysis of *obd* SIVP vessel angiogenesis. (I) Measurement of the area of the vessel coverage over the yolk of wild-type and *obd* mutant embryos at 55 hpf. J) The mean number of compartments per SIVP in wild-type and *obd* mutant embryos was calculated at 55 hpf. The average values were calculated and plotted in a graph. $^{**}=p \leq 0.01$ and $^{***}=p \leq 0.001$ by the Student's *T*-Test. Scale bars represent 100 μm.

of DMH1 was functional, we exposed siblings of the experimental embryos to DMH1 from 4 hpf observing dorsalizing effects as shown in Hao et al., 2010 (Fig. S5). Moreover, injection of *bmp4* morpholino phenocopied the treatment with DMH1 suggesting that Bmp4 is a positive cue for growth (Fig. 8D–D′). Using our quantitative analysis, we found a decreased area, decreased number of endothelial cells, but no significant difference in the number of basket compartments with Bmp inhibition (Fig. 8L–N).

Vascular endothelial growth factors are critically important in blood vessel formation (Liang et al., 2001). For this reason we investigated the role of VegfA on SIVP formation treating the embryos with a Vegfr2 inhibitor (DMH4, Hao et al., 2010). If 50 μM DMH4 is applied at 4 hpf, there is a complete lack of SIVP formation (Fig. 9A–A″). However, when the drug is applied from 24 hpf, embryos show an absence of SIVP compartments, but still have a lumenized, external SIVP vessel present (Fig. 8E–E′). Moreover, continued drug exposure through 3 dpf did not allow any additional sprouting (data not shown). Proper patterning is not recovered after removing the drug, suggesting there is a critical early window for sprouting from the vein to form the SIVP. These data suggest that the program for development of the first SIVP sprout to form the outer vessel of the SIVP is determined before 24 hpf and together with the formation of derivative sprouts, it is Vegf-dependent.

Using our quantitative analysis on 50 μM DMH4 treated embryos from 24 hpf, we found no change in area of the SIVP, but there was a strongly decreased number of endothelial cells, and a large decrease in the number of basket compartments (Fig. 8L–N). These data suggest that expansion and migration of the first, outer SIVP vessel is not Vegf-dependent at later timepoints. As a positive control, we showed that other angiogenic beds are inhibited with

this drug; the central arteries in the head (CtAs) sprout at the same time as the SIVP and are not present in DMH4 treated embryos (Fig. S6). In support of the Vegf playing a role in SIVP development, *vegfaa* and *vegfab* (the two *vegfA* isoforms) are expressed in the podocytes of the pronephric ducts adjacent to the developing SIVP and *vegfr2* is expressed by SIVP endothelial cells (Fig. S1). Others have also reported that *vegfA* is expressed in the developing pro-nephros/podocytes (Liang et al., 2001; Majumdar et al., 2000). Morpholino knockdown of *vegfaa* does not show SIVP phenotype but knockdown of *vegfab* morpholino strongly reduces the SIVP basket (Fig. 8F–G′). Double knockdown of *vegfaa* and *vegfab* does not show an additional phenotype (Fig. 8H–H′).

Since inhibition of Vegf or Bmp signaling both interfere with SIVP formation, this suggests that both pathways contribute to its development. We next wanted to understand whether Vegf and Bmp work in parallel pathways to influence SIVP angiogenesis. We inhibited both pathways simultaneously using either a single drug that blocks both receptors (dorsomorphin) or two drugs that are specific for either receptor (DMH4 and DMH1). Double knockdown eliminates the SIVP and suggests that Vegf and Bmp act in parallel and have partially overlapping roles in promoting SIVP sprouting and growth (Fig. 8I–J′). The Mek/Erk pathway is also downstream of Bmp and Vegf pathways as shown in zebrafish CVP development. We inhibited Mek-1 and -2 through use of 30 μM SL327 (Wiley et al., 2011) and found that the SIVP is also almost completely eliminated (Fig. 8K–K′). As a positive control, we show that the drug also disrupts CVP formation (Wiley et al. 2011; Fig. S6).

Thus our screen for growth factor pathways affecting SIVP development suggests that Vegf and Bmp act in parallel to promote SIVP development, with Vegf promoting initial sprouting and inner vessel formation and Bmp promoting outgrowth over the yolk.
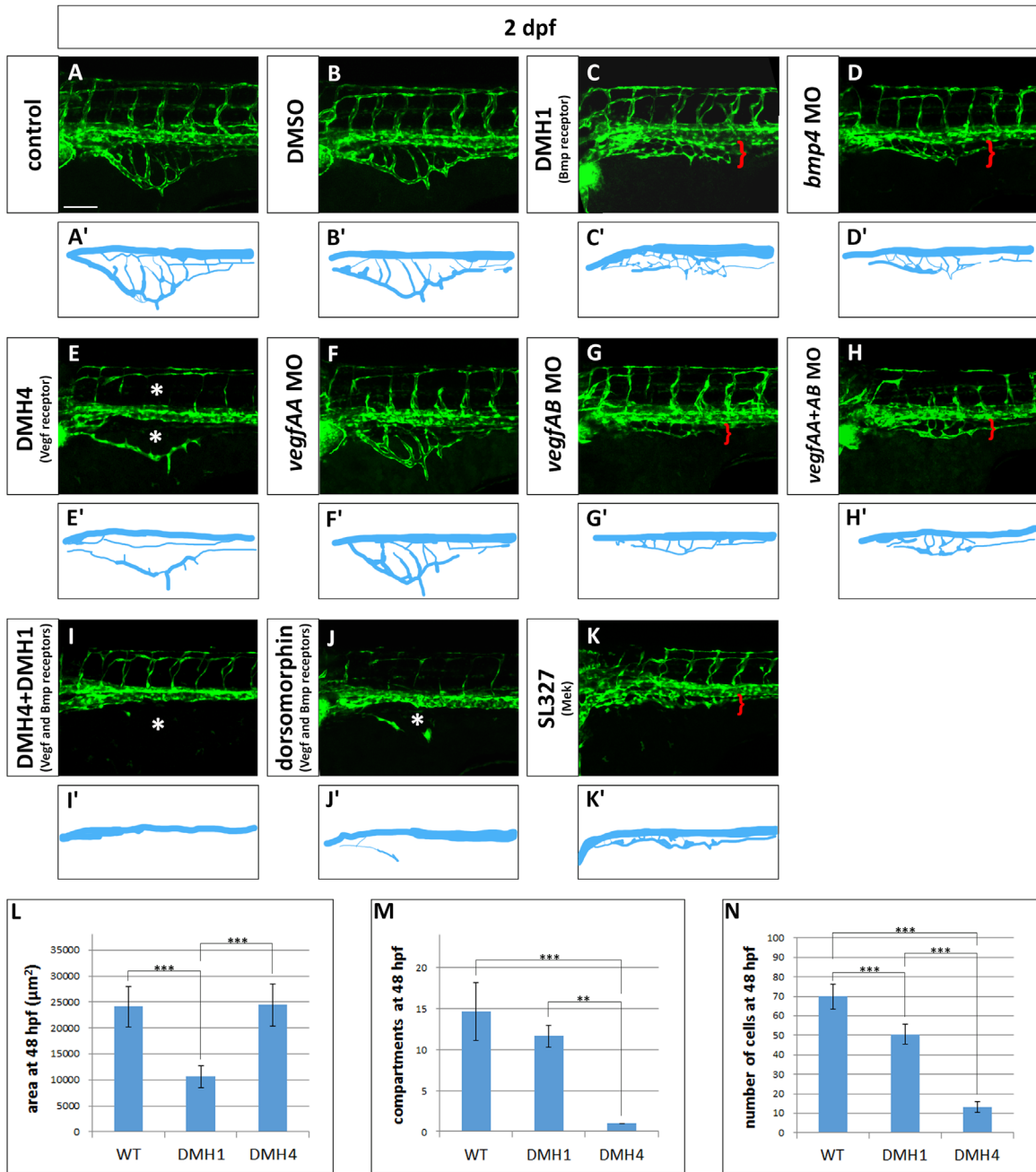
Fig. 8. Vegf and Bmp redundantly control SIVP growth. (A–K) Phenotype of embryos treated with small molecule inhibitors from 24 hpf to 48 hpf or morpholinos. (A) Untreated control embryo (B) DMSO treated control embryos. (C) 50 μM DMH1 treated embryo, an inhibitor of the Bmp type I receptor Alk2. (D) *bmp4* morphant. (E) 50 μM DMH4 treated embryo, a Vegfr2 inhibitor. (F) *vegfaa* morphant. (G) *vegfab* morphant. (H) *vegfaa* and *vegfab* double morphants. (I) DMH4 and DMH1 treated embryo at 25 μM each. (J) 50 μM dorsomorphin. (K) 30 μM SL327, a Mek-1/Mek-2 inhibitor. (A′–K′) Schematics corresponding to images above (A–K). Red brackets indicate the reduced expansion of the SIVP and asterisks mark the absence of SIVP internal vessels and ISVs. Scale bar represents 100 μm. (L–N) Measurement of the average area of the vessel coverage over the yolk, number of compartments or number of cells at 48 hpf for wild-type, DMH1 treated and DMH4 treated embryos. $^{**}=p \leq 0.01$ and $^{***}=p \leq 0.001$ using ANOVA.

Other pathways important for arterial angiogenesis, including Notch, Sonic Hedgehog and Pdgf, appear not to be important for formation of this vessel bed.

3.9. *obd* embryos have decreased sensitivity to Vegf inhibition

obd mutants have abnormal Vegf signaling with decreased sFlt1 expression and therefore higher Vegfr2 activity (Zygmunt et al., 2011). In order to understand this relationship during SIVP development, we blocked Vegf signaling in wild-type and *obd* mutant embryos using DMH4 from 4 or from 24 hpf (Fig. 9). When

we inhibit Vegfr2 action in wild-type embryos from 4 hpf we see significantly decreased sprouting from the PCV, with only one aberrant sprout from the duct of Cuvier persisting during this window. This sprout was limited in extension (Fig. 9A–A″). As previously noted, when treated from 24 hpf with DMH4, wild-type embryos only show the external SIVP vessel with no compartments or connections to the supraintestinal artery (Fig. 9B–B″). In *obd* mutant embryos when we treat with DMH4 from 4 hpf we observe some sprouts from the PCV when there are none in wild-type treated embryos. While these sprouts do not migrate extensively over the yolk, they are still present during Vegf blockade,
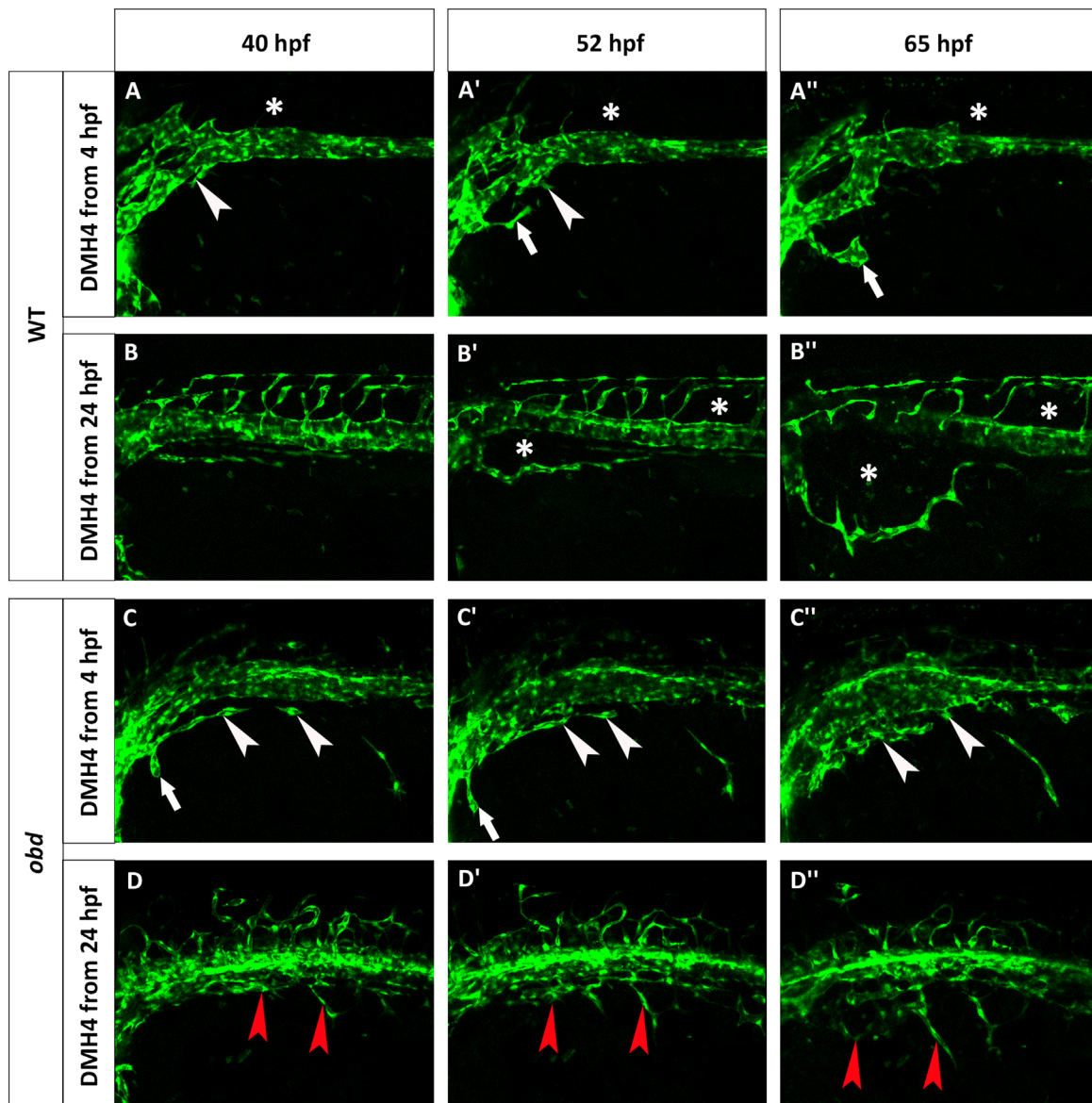
Fig. 9. *obd* mutants are less sensitive to Vegf inhibition. Phenotype of wild-type (A–B″) and *obd* (C–D″) embryos treated with 50 μM DMH4. (A–A″) A *Tg(fli:EGFP)^y1* wild-type was treated from 4 hpf and lacks the first SIVP sprouts. White arrowheads point to the attempted sprouts from along the PCV. White arrows indicate an aberrant sprout from the duct of Cuvier. (B–B″) A *Tg(fli:EGFP)^y1* wild-type was treated from 24 hpf which stops the formation of SIVP vascular compartments. Asterisks mark the absence of the internal vessels and dysmorphic ISVs. The expansion of the external vessel above the yolk ball is not affected by the inhibition. (C–C″) *obd^fov01b*; *Tg(fli:EGFP)^y1* treated embryo from 4 hpf shows some sprouts are present. White arrowheads indicate blocked sprouts from along the vein. White arrows point to irregular sprouts from the duct of Cuvier. (D–D″) *obd^fov01b*; *Tg(fli:EGFP)^y1* embryo treated from 24 hpf. Red arrowheads point to residual sprouts. Scale bars represent 100 μm.

suggesting persistence of a sprouting program (compare Fig. 9A–A″ and C–C″). Drug treatment from 24 hpf has a similar effect on *obd* embryos in reducing, but not completely eliminating sprouts (Fig. 9D–D″). In contrast, DMH4 treatment from 24 hpf in wild-type embryos allowed only the first external SIVP vessel to develop properly (Fig. 8 and Fig. 9B–B″). In wild-type embryos, morpholino knockdown of *vegfab* but not *vegfaa* inhibits SIVP development (Fig. 8). In *obd* mutants, *vegfab* also appears to be the more important *vegfA* gene for SIVP development (Fig. S7).

obd mutants are also sensitive to Bmp signaling inhibition. Treatment with DMH1 reduced the SIVP expansion in *obd* embryos (Fig. S7) and double inhibition of Vegf and Bmp pathway drastically reduces SIVP development in *obd* mutants although there are a few residual sprouts that are not inhibited (Fig. S7). Inhibition of Mek/Erk signaling also reduces, but not completely eliminates, SIVP development (Fig. S7).

4. Discussion

The intent of this project was to understand the anatomical and molecular basis of visceral venous plexus formation. The developing SIVP is easily visible and accessible to manipulation and is a popular model for pro- and anti-angiogenesis drug screening (Chan et al., 2012; Kuo et al., 2011; Raghunath et al., 2009; Serbedzija et al., 1999) and cancer models (Nicoli et al., 2009, 2007; Nicoli and Presta, 2007). Some of our results, however call into question the use of this model for drug screening without taking into account that this plexus responds to a different set of molecular cues than those that influence arterial vessel bed development.

The SIVP is directly above YSL, an important early developmental signaling center that absorbs nutrients from the yolk and transports them to the embryo (reviewed in Carvalho and Heisenberg, 2010). Moreover, the YSL expresses genes required in

early metabolism and nutrition, such as lipid metabolism, long before the embryo is capable of sustaining feeding and absorption. The zebrafish SIVP is structurally and functionally homologous to the murine vitelline veins, transporting nutrients from the mother's body through the yolk sac to the developing embryo.

Previous observations suggested that the duct of Cuvier as the source and origin of the first SIVP sprout (Isogai et al., 2001; Nicoli and Presta, 2007), however, with the use of time-lapse imaging we demonstrate that the source of angioblasts is actually the PCV. These cells sprout from different positions along the axial vein and migrate ventrally to join with each other. They then form a basket that runs from the yolk to the posterior end of the yolk extension. During the revision of this paper, both (Lenard et al., 2015) and (Nicenboim et al., 2015) published a similar analysis of SIVP formation. These two research teams suggest the SIVP is derived from the PCV. Nicenboim and colleagues also used lineage tracing to demonstrate that the SIVP is generated from asymmetric cell divisions from the posterior cardinal vein.

The intersegmental vessels are a well characterized model for angiogenesis because of their simplicity and stereotypical patterning. These primary angiogenic vessels sprout from both sides of the dorsal aorta, grow dorsally following the vertical boundary between somites and join together into the dorsal longitudinal anastomotic vessel dorsal to the neural tube (Childs et al., 2002). However, many mammalian vessel beds develop from non-stereotypical vascular plexuses, more similar to SIVP formation. In this type of angiogenesis, the initial vascular plexus contains more vessels than necessary and is subsequently remodeled into an efficient vascular network. The SIVP is venous in its initial formation, which also distinguishes it from the ISVs that initially sprout from the aorta (Isogai et al., 2003). The variability in pattern among embryos in the SIVP suggests that angioblast migration does not follow a pre-determined spatial pattern of molecular cues. However, given that we were able to obtain a staging series with characteristic growth parameters, this suggests there is some control of migration and pattern. In this way, the SIVP is similar to the midbrain vasculature, which also does not develop with a fixed pattern but resolves into a patterned network (Chen et al., 2012).

In addition to the previously described superficial SIVP, we observe that there is an inner, smaller and denser vascular plexus underneath the earlier forming SIVP basket. The inner SIVP basket wraps the anterior part of the digestive system and has the same morphology as the superficial SIVP on the yolk with an outer vessel and compartments branching from it. We were able to see common vessels between the two baskets suggesting shared blood flow. Since the outer basket regresses during later embryonic development, this suggests that the inner basket gradually takes over from the outer basket as the yolk depletes, and is the vascular bed specialized in absorbing and distributing nutrition from the gut. The developing gut is a source of Bmp that likely promotes the development of the adjacent SIVP (Zeng and Childs, 2012).

During SIVP development we were able to pinpoint key common steps. The presence of filopodia and lamellipodia suggests active migration of angioblasts and an active scan of the environment for attractive or repulsive cues during migration. We observed *vegfA* expression in the pronephric ducts and *bmp4* in the gut, and both are required for SIVP angiogenesis. Interestingly, we also observed remodeling and pruning events similar to those seen in the mature midbrain vasculature, which are of critical importance for the efficiency of circulation (Chen et al., 2012). Lenard et al. (2015) also recently showed the pruning process in the SIVP follows the opposite sequence of events that occur in anastomosis (Lenard et al., 2015).

In order to be able to compare SIVP development in mutants, we measured quantitative features of SIVP development. The speed of migration of the leading sprouts of the SIVP was 4.5 μm/h

which is slightly slower than what is observed for cultured primary endothelial cells that migrate up to 15 μm/h (Vitorino and Meyer, 2008). In comparison, ISV migration in zebrafish has an average speed of 17 μm/h that steadily decreases over 3 h post-sprouting, then increases again to around 10 μm/h at 5 hours post-initiation (Shirinifard et al., 2013). Thus the SIVP migrates slightly slower than other vessel types *in vitro* and *in vivo*.

We also observed that both leading (tip) and trailing (stalk) cells proliferate during SIVP expansion, which contrasts to the ISVs where tip but not stalk cells proliferate (Siekmann and Lawson, 2007), or mouse retinal vessels where stalk but not tip cells proliferate (Gerhardt et al., 2003). We did not observe any directionality in the plane of cell division during this process.

We were curious to look for a role of PlexinD1 in SIVP development. *plexinD1* is highly expressed in normal vascular endothelium. Activation of PlexinD1 causes filopodial collapse to halt angioblast migration in the direction of the repulsive cue. *obd* mutants show exuberant vessel growth in both the ISVs and SIVP, highlighting a role for PlexinD1 in suppressing both arterial and venous sprouting and migration. We observed increased migration and number of smaller vessels making compartments as well as reduced pruning events in *obd* mutants. *obd* mutants have an increased number of endothelial cells in the ISVs (Zygmunt et al., 2011) as well as in the SIVP. Thus, PlexinD1 plays a similar role in both ISV and SIVP development to control spatial and temporal sprouting and vascular patterning. Given the relationship between PlexinD1 and Vegf, it is not surprising that *obd* mutants are also less sensitive to Vegf blockade during SIVP development.

We were surprised that when we explored the roles of known angiogenic growth factors, only Vegf and Bmp pathways play a role in SIVP development, while Shh, Notch and Pdgfr were dispensable. Vegf inhibition blocks all formation of the SIVP if administered at early timepoints. Vegf is also necessary for inner compartment formation, most likely through its role in promoting proliferation as the number of SIVP cells is substantially decreased in the absence of Vegf signaling. It is interesting that the outermost SIVP vessel still migrates to a normal position on the yolk when we inhibit Vegfr2 later in development. This suggests that migration of the SIVP over the yolk is not controlled by Vegf signaling.

On the other hand, Bmp, which promotes ventral sprouting during CVP development (Wakayama et al., 2015; Wiley et al., 2011), is expressed in the adjacent gut during SIVP development (Zeng and Childs, 2012). The SIVP has strongly reduced expansion in the absence of Bmp signaling. Thus, analogous to its role in the CVP, Bmp promotes migration or outgrowth of the SIVP. However unlike the CVP, Bmp is not necessary for initial sprouting. Vegf and Bmp therefore play distinct but partially overlapping roles in patterning this venous structure suggesting a partial redundancy. The double inhibition of Vegf and Bmp pathway completely blocks the formation of the SIVP confirming that the two pathways are necessary and sufficient to control the proper formation of this venous bed (see schematics in Fig. 10). Vegf is not involved in CVP development, while it is involved in SIVP development, which is a distinction between the patterning of these two vessel beds.

A molecular connection between the Vegf and PlexinD1 pathways has been reported via the induction of *sflt1* expression by PlexinD1 (Zygmunt et al., 2011) during ISV formation. sFlt1 sequesters VegfA reducing the activation of the signaling cascade downstream of Vegfr2. Since loss of PlexinD1 leads to decreased inhibitory decoy receptor expression and therefore increased VegfA availability to signal through Vegfr2, we reasoned that vessel overgrowth in *obd* mutants should be sensitive to Vegfr2 inhibition. Interestingly, Vegfr2 inhibition was less effective in *obd* mutants as compared to wild-type embryos, perhaps reflecting the higher concentrations of available VegfA to bind to Vegfr2.
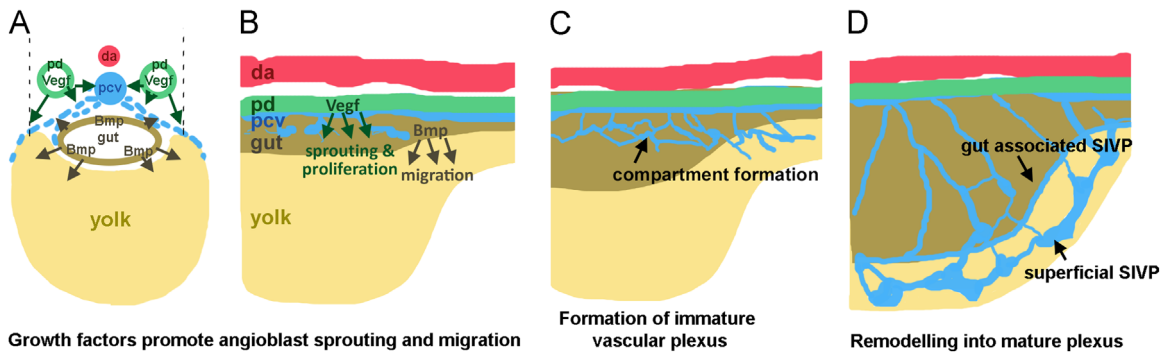
Fig. 10. Model of SIVP development. In cross section and lateral view at early stages (A–B), Vegf is secreted by the pronephric ducts (green) while Bmp is secreted by the intestine (brown). VegfA (green arrows), promotes sprouting of cells to form the SIVP from the posterior cardinal vein (pcv, blue). Bmp4 expressed in the gut (brown arrows), promotes the migration of angioblasts from the vein. (C) At later stages, honeycomb-structured vascular compartments form. (D) The mature plexus comprises a remodeled inner and outer basket. Abbreviations: da (red): dorsal aorta; pd (green): pronephric duct; pcv (blue): posterior cardinal vein; (brown): gut; (yellow): yolk.

Given the differences between SIVP formation and ISV formation, the use of the SIVP as a system to test pro- and anti-angiogenic drugs or cancer angiogenesis needs to be carefully considered. Our study will be a useful tool to understand the specific action of new drugs provided they are considered within the context of wild-type development. For instance, patterning is highly variable, and studies that use growth parameters need to include enough embryos to fully assess variability in the wild-type and experimental population. Furthermore, the different sensitivity of the SIVP to growth factor inhibition (insensitive to Notch, Shh or Pdgf inhibition, but sensitive to Vegf and Bmp inhibition) contrasts to other vascular beds. Screening for anti-angiogenic molecules in this bed will therefore yield different targets than if other vessel beds were studied. This could be both a strength and weakness of the system. We propose that the developing gut vasculature is a unique model to shed insight into novel mechanisms utilized in venous and organ-specific angiogenesis.

Appendix A. Supplementary material

Supplementary data associated with this article can be found in the online version at http://dx.doi.org/10.1016/j.ydbio.2015.10.017.

References

Avraham-Davidi, I., Ely, Y., Pham, V.N., Castranova, D., Grunspan, M., Malkinson, G., Gibbs-Bar, L., Mayseless, O., Allmog, G., Lo, B., Warren, C.M., Chen, T.T., Ungos, J., Kidd, K., Shaw, K., Rogachev, I., Wan, W., Murphy, P.M., Farber, S.A., Carmel, L., Shelness, G.S., Iruela-Arispe, M.L., Weinstein, B.M., Yaniv, K., 2012. ApoB-containing lipoproteins regulate angiogenesis by modulating expression of VEGF receptor 1. Nat. Med. 18, 967–973.

Bahary, N., Goishi, K., Stuckenholz, C., Weber, G., Leblanc, J., Schafer, C.A., Berman, S. S., Klagsbrun, M., Zon, L.I., 2007. Duplicate VegfA genes and orthologues of the KDR receptor tyrosine kinase family mediate vascular development in the zebrafish. Blood 110, 3627–3636.

Ben Shoham, A., Malkinson, G., Krief, S., Shwartz, Y., Ely, Y., Ferrara, N., Yaniv, K., Zelzer, E., 2012. S1P1 inhibits sprouting angiogenesis during vascular development. Development 139, 3859–3869.

Carmeliet, P., Ferreira, V., Breier, G., Pollefeyt, S., Kieckens, L., Gertsenstein, M., Fahrig, M., Vandenhoeck, A., Harpal, K., Eberhardt, C., Declercq, C., Pawling, J., Moons, L., Collen, D., Risau, W., Nagy, A., 1996. Abnormal blood vessel development and lethality in embryos lacking a single VEGF allele. Nature 380, 435–439.

Carvalho, L., Heisenberg, C.P., 2010. The yolk syncytial layer in early zebrafish development. Trends Cell Biol. 20, 586–592.

Chan, Y.K., Kwok, H.H., Chan, L.S., Leung, K.S., Shi, J., Mak, N.K., Wong, R.N., Yue, P.Y., 2012. An indirubin derivative, E804, exhibits potent angiosuppressive activity. Biochem. Pharmacol. 83, 598–607.

Chen, Q., Jiang, L., Li, C., Hu, D., Bu, J.W., Cai, D., Du, J.L., 2012. Haemodynamics-driven developmental pruning of brain vasculature in zebrafish. PLoS Biol. 10, e1001374.

Childs, S., Chen, J.N., Garrity, D.M., Fishman, M.C., 2002. Patterning of angiogenesis in the zebrafish embryo. Development 129, 973–982.

Choi, J., Mouillesseaux, K., Wang, Z., Fiji, H.D., Kinderman, S.S., Otto, G.W., Geisler, R., Kwon, O., Chen, J.N., 2011. Aplexone targets the HMG–CoA reductase pathway and differentially regulates arteriovenous angiogenesis. Development 138, 1173–1181.

Covassin, L.D., Villefranc, J.A., Kacergis, M.C., Weinstein, B.M., Lawson, N.D., 2006. Distinct genetic interactions between multiple Vegf receptors are required for development of different blood vessel types in zebrafish. Proc. Natl. Acad. Sci. USA 103, 6554–6559.

Crawford, L.W., Foley, J.F., Elmore, S.A., 2010. Histology atlas of the developing mouse hepatobiliary system with emphasis on embryonic days 9.5–18.5. Toxicol. Pathol. 38, 872–906.

Donovan, A., Brownlie, A., Zhou, Y., Shepard, J., Pratt, S.J., Moynihan, J., Paw, B.H., Drejer, A., Barut, B., Zapata, A., Law, T.C., Brugnara, C., Lux, S.E., Pinkus, G.S., Pinkus, JL., Kingsley, P.D., Palis, J., Fleming, M.D., Andrews, N.C., Zon, L.I., 2000. Positional cloning of zebrafish ferroportin1 identifies a conserved vertebrate iron exporter. Nature 403 (6771), 776–781.

Fouquet, B., Weinstein, B.M., Serluca, F.C., Fishman, M.C., 1997. Vessel patterning in the embryo of the zebrafish: guidance by notochord. Dev. Biol. 183, 37–48.

Gay, C.M., Zygmunt, T., Torres-Vazquez, J., 2011. Diverse functions for the semaphorin receptor PlexinD1 in development and disease. Dev. Biol. 349, 1–19.

Gerhardt, H., Golding, M., Fruttiger, M., Ruhrberg, C., Lundkvist, A., Abramsson, A., Jeltsch, M., Mitchell, C., Alitalo, K., Shima, D., Betsholtz, C., 2003. VEGF guides angiogenic sprouting utilizing endothelial tip cell filopodia. J. Cell Biol. 161, 1163–1177.

Geudens, I., Gerhardt, H., 2011. Coordinating cell behaviour during blood vessel formation. Development 138, 4569–4583.

Hao, J., Ho, JN., Lewis, JA., Karim, K.A., Daniels, R.N., Gentry, P.R., Hopkins, C.R., Lindsley, C.W., Hong, C.C., 2010. In vivo structure–activity relationship study of dorsomorphin analogues identifies selective VEGF and BMP inhibitors. ACS Chem. Biol 5 (2), 245–253. http://dx.doi.org/10.1021/cb9002865.

Helker, C.S., Schuermann, A., Karpanen, T., Zeuschner, D., Belting, H.G., Affolter, M., Schulte-Merker, S., Herzog, W., 2013. The zebrafish common cardinal veins develop by a novel mechanism: lumen ensheathment. Development 140, 2776–2786.

Hogan, B.M., Bos, F.L., Bussmann, J., Witte, M., Chi, N.C., Duckers, H.J., Schulte-Merker, S., 2009a. Ccbe1 is required for embryonic lymphangiogenesis and venous sprouting. Nat. Genet. 41, 396–398.

Hogan, B.M., Herpers, R., Witte, M., Helotera, H., Alitalo, K., Duckers, H.J., Schulte-Merker, S., 2009b. Vegfc/Flt4 signalling is suppressed by Dll4 in developing zebrafish intersegmental arteries. Development 136, 4001–4009.

Hussain, M.M., Rava, P., Pan, X., Dai, K., Dougan, S.K., Iqbal, J., Lazare, F., Khatun, I., 2008. Microsomal triglyceride transfer protein in plasma and cellular lipid metabolism. Curr. Opin. Lipidol. 19, 277–284.

Isogai, S., Horiguchi, M., Weinstein, B.M., 2001. The vascular anatomy of the developing zebrafish: an atlas of embryonic and early larval development. Dev.

Biol. 230, 278–301.

Isogai, S., Lawson, N.D., Torrealday, S., Horiguchi, M., Weinstein, B.M., 2003. Angiogenic network formation in the developing vertebrate trunk. Development 130, 5281–5290.

Kaufman, M.H., 1999a. The Atlas of Mouse Development. Academic Press, San Diego, CA.

Kaufman, M.H., Bard, J.B.L., 1999b. The Anatomical Basis of Mouse Development. Academic Press, San Diego.

Kedinger, M., Duluc, I., Fritsch, C., Lorentz, O., Plateroti, M., Freund, J.N., 1998. Intestinal epithelial-mesenchymal cell interactions. Ann. NY Acad. Sci. 859, 1–17.

Kendall, R.L., Thomas, K.A., 1993. Inhibition of vascular endothelial cell growth factor activity by an endogenously encoded soluble receptor. Proc. Natl. Acad. Sci. USA 90, 10705–10709.

Kim, J., Oh, W.J., Gaiano, N., Yoshida, Y., Gu, C., 2011. Semaphorin 3E-Plexin-D1 signaling regulates VEGF function in developmental angiogenesis via a feedback mechanism. Genes Dev. 25, 1399–1411.

Kuo, M.W., Wang, C.H., Wu, H.C., Chang, S.J., Chuang, Y.J., 2011. Soluble THSD7A is an N-glycoprotein that promotes endothelial cell migration and tube formation in angiogenesis. PLoS One 6, e29000.

Lamont, R.E., Vu, W., Carter, A.D., Serluca, F.C., MacRae, C.A., Childs, S.J., 2010. Hedgehog signaling via angiopoietin1 is required for developmental vascular stability. Mech Dev 127 (3–4), 159–168. http://dx.doi.org/10.1016/j.mod.2010.02.001.

Lauter, G., Soll, I., Hauptmann, G., 2011. Two-color fluorescent in situ hybridization in the embryonic zebrafish brain using differential detection systems. BMC Dev. Biol. 11, 43.

Lawson, N.D., Vogel, A.M., Weinstein, B.M., 2002. Sonic hedgehog and vascular endothelial growth factor act upstream of the notch pathway during arterial endothelial differentiation. Dev. Cell 3, 127–136.

Lawson, N.D., Weinstein, B.M., 2002. In vivo imaging of embryonic vascular development using transgenic zebrafish. Dev. Biol. 248, 307–318.

Lenard, A., Daetwyler, S., Betz, C., Ellertsdottir, E., Belting, H.G., Huisken, J., Affolter, M., 2015. Endothelial cell self-fusion during vascular pruning. PLoS Biol. 13, e1002126.

Liang, D., Chang, J.R., Chin, A.J., Smith, A., Kelly, C., Weinberg, E.S., Ge, R., 2001. The role of vascular endothelial growth factor (VEGF) in vasculogenesis, angiogenesis, and hematopoiesis in zebrafish development. Mech. Dev. 108, 29–43.

Majumdar, A., Lun, K., Brand, M., Drummond, I.A., 2000. Zebrafish no isthmus reveals a role for pax2.1 in tubule differentiation and patterning events in the pronephric primordia. Development 127, 2089–2098.

Marza, E., Barthe, C., Andre, M., Villeneuve, L., Helou, C., Babin, P.J., 2005. Developmental expression and nutritional regulation of a zebrafish gene homologous to mammalian microsomal triglyceride transfer protein large subunit. Dev. Dyn. 232, 506–518.

Mendelson, K., Zygmunt, T., Torres-Vazquez, J., Evans, T., Hla, T., 2013. Sphingosine 1-phosphate receptor signaling regulates proper embryonic vascular patterning. J. Biol. Chem. 288, 2143–2156.

Nicenboim, J., Malkinson, G., Lupo, T., Asaf, L., Sela, Y., Mayseless, O., Gibbs-Bar, L., Senderovich, N., Hashimshony, T., Shin, M., Jerafi-Vider, A., Avraham-Davidi, I., Krupalnik, V., Hofi, R., Almog, G., Astin, J.W., Golani, O., Ben-Dor, S., Crosier, P.S., Herzog, W., Lawson, N.D., Hanna, J.H., Yanai, I., Yaniv, K., 2015. Lymphatic vessels arise from specialized angioblasts within a venous niche. Nature 522, 56–61.

Nicoli, S., De Sena, G., Presta, M., 2009. Fibroblast growth factor 2-induced angiogenesis in zebrafish: the zebrafish yolk membrane (ZFYM) angiogenesis assay. J. Cell. Mol. Med. 13, 2061–2068.

Nicoli, S., Presta, M., 2007. The zebrafish/tumor xenograft angiogenesis assay. Nat. Protoc. 2, 2918–2923.

Nicoli, S., Ribatti, D., Cotelli, F., Presta, M., 2007. Mammalian tumor xenografts induce neovascularization in zebrafish embryos. Cancer Res. 67, 2927–2931.

Nishioka, C., Ikezoe, T., Yang, J., Miwa, A., Tasaka, T., Kuwayama, Y., Togitani, K., Koeffler, H.P., Yokoyama, A., 2008. Ki11502, a novel multitargeted receptor tyrosine kinase inhibitor, induces growth arrest and apoptosis of human leukemia cells in vitro and in vivo. Blood 111, 5086–5092.

Okuda, K.S., Astin, J.W., Misa, J.P., Flores, M.V., Crosier, K.E., Crosier, P.S., 2012. lyve1 expression reveals novel lymphatic vessels and new mechanisms for lymphatic vessel development in zebrafish. Development 139, 2381–2391.

Raghunath, M., Sy Wong, Y., Farooq, M., Ge, R., 2009. Pharmacologically induced angiogenesis in transgenic zebrafish. Biochem. Biophys. Res. Commun. 378, 766–771.

Ramalho-Santos, M., Melton, D.A., McMahon, A.P., 2000. Hedgehog signals regulate multiple aspects of gastrointestinal development. Development 127, 2763–2772.

Roberts, D.J., Smith, D.M., Goff, D.J., Tabin, C.J., 1998. Epithelial-mesenchymal signaling during the regionalization of the chick gut. Development 125, 2791–2801.

Roberts, D.M., Kearney, J.B., Johnson, J.H., Rosenberg, M.P., Kumar, R., Bautch, V.L., 2004. The vascular endothelial growth factor (VEGF) receptor Flt-1 (VEGFR-1) modulates Flk-1 (VEGFR-2) signaling during blood vessel formation. Am. J. Pathol. 164, 1531–1535.

Roman, B.L., Pham, V.N., Lawson, N.D., Kulik, M., Childs, S., Lekven, A.C., Garrity, D. M., Moon, R.T., Fishman, M.C., Lechleider, R.J., Weinstein, B.M., 2002. Disruption of acvrl1 increases endothelial cell number in zebrafish cranial vessels. Development 129, 3009–3019.

Sakurai, A., Gavard, J., Annas-Linhares, Y., Basile, J.R., Amornphimoltham, P., Palmby, T.R., Yagi, H., Zhang, F., Randazzo, P.A., Li, X., Weigert, R., Gutkind, J.S., 2010. Semaphorin 3E initiates antiangiogenic signaling through plexin D1 by regulating Arf6 and R-Ras. Mol. Cell. Biol. 30, 3086–3098.

Schindelin, J., Arganda-Carreras, I., Frise, E., Kaynig, V., Longair, M., Pietzsch, T., Preibisch, S., Rueden, C., Saalfeld, S., Schmid, B., Tinevez, J.Y., White, D.J., Hartenstein, V., Eliceiri, K., Tomancak, P., Cardona, A., 2012. Fiji: an open-source platform for biological-image analysis. Nat. Methods 9, 676–682.

Serbedzija, G.N., Flynn, E., Willett, C.E., 1999. Zebrafish angiogenesis: a new model for drug screening. Angiogenesis 3, 353–359.

Shalaby, F., Rossant, J., Yamaguchi, T.P., Gertsenstein, M., Wu, X.F., Breitman, M.L., Schuh, A.C., 1995. Failure of blood-island formation and vasculogenesis in Flk-1-deficient mice. Nature 376, 62–66.

Shirinifard, A., McCollum, C.W., Bolin, M.B., Gustafsson, J.A., Glazier, J.A., Clendenon, S.G., 2013. 3D quantitative analyses of angiogenic sprout growth dynamics. Dev. Dyn. 242, 518–526.

Siekmann, A.F., Lawson, N.D., 2007. Notch signalling limits angiogenic cell behaviour in developing zebrafish arteries. Nature 445, 781–784.

Torres-Vazquez, J., Gitler, A.D., Fraser, S.D., Berk, J.D., Van, N.P., Fishman, M.C., Childs, S., Epstein, J.A., Weinstein, B.M., 2004. Semaphorin-plexin signaling guides patterning of the developing vasculature. Dev. Cell 7, 117–123.

Vitorino, P., Meyer, T., 2008. Modular control of endothelial sheet migration. Genes Dev. 22, 3268–3281.

Wakayama, Y., Fukuhara, S., Ando, K., Matsuda, M., Mochizuki, N., 2015. Cdc42 mediates bmp-induced sprouting angiogenesis through Fmnl3-driven assembly of endothelial filopodia in zebrafish. Dev. Cell 32, 109–122.

Wallace, K.N., Pack, M., 2003. Unique and conserved aspects of gut development in zebrafish. Dev. Biol. 255, 12–29.

Wiens, K.M., Lee, H.L., Shimada, H., Metcalf, A.E., Chao, M.Y., Lien, C.L., 2010. Platelet-derived growth factor receptor beta is critical for zebrafish intersegmental vessel formation. PLoS One 5, e11324.

Wiley, D.M., Kim, J.D., Hao, J., Hong, C.C., Bautch, V.L., Jin, S.W., 2011. Distinct signalling pathways regulate sprouting angiogenesis from the dorsal aorta and the axial vein. Nat. Cell. Biol. 13, 686–692.

Yaniv, K., Isogai, S., Castranova, D., Dye, L., Hitomi, J., Weinstein, B.M., 2006. Live imaging of lymphatic development in the zebrafish. Nat. Med. 12, 711–716.

Zeng, L., Childs, S.J., 2012. The smooth muscle microRNA miR-145 regulates gut epithelial development via a paracrine mechanism. Dev. Biol. 367, 178–186.

Zygmunt, T., Gay, C.M., Blondelle, J., Singh, M.K., Flaherty, K.M., Means, P.C., Herwig, L., Krudewig, A., Belting, H.G., Affolter, M., Epstein, J.A., Torres-Vazquez, J., 2011. Semaphorin-PlexinD1 signaling limits angiogenic potential via the VEGF decoy receptor sFlt1. Dev. Cell 21, 301–314.